

1 Title: Comparative genomics on cultivated and uncultivated, freshwater and marine *Candidatus*
2 Manganitrophaceae species implies their worldwide reach in manganese chemolithoautotrophy

3

4 Running title: Phylogenomics of manganese-oxidizing *Nitrospirota*

5

6 Keywords: autotroph, lithotroph, chemolithoautotroph, manganese oxide, manganese carbonate,
7 Nitrospirae, Nitrospirota, Mn, Mn²⁺, Mn(II), Mn (II)

8

9 Authors: Hang Yu^a, Grayson L. Chadwick^a, Usha F. Lingappa^a, Jared R. Leadbetter^{a,b}

10

11 ^aDivision of Geological & Planetary Sciences and ^bDivision of Engineering & Applied Science,
12 California Institute of Technology, Pasadena, CA, USA 91125

13

14 Correspondence: Hang Yu (hyu@caltech.edu) and Jared R. Leadbetter (jleadbetter@caltech.edu)

15

16 **Abstract**

17 Chemolithoautotrophic manganese oxidation has long been theorized, but only recently
18 demonstrated in a bacterial co-culture. The majority member of the co-culture, *Candidatus*
19 *Manganitrophus noduliformans*, is a distinct but not yet isolated lineage in the phylum *Nitrospirota*
20 (*Nitrospirae*). Here, we established two additional MnCO₃-oxidizing cultures using inocula from
21 Santa Barbara (USA) and Boetsap (South Africa). Both cultures were dominated by strains of a
22 new species, designated *Candidatus Manganitrophus morganii*. The next abundant members
23 differed in the available cultures, suggesting that while *Ca. Manganitrophus* species have not been
24 isolated in pure culture, they may not require a specific syntrophic relationship with another
25 species. Phylogeny of cultivated *Ca. Manganitrophus* and related metagenome-assembled
26 genomes revealed a coherent taxonomic family, *Candidatus Manganitrophaceae*, from both
27 freshwater and marine environments and distributed globally. Comparative genomic analyses
28 support this family being Mn(II)-oxidizing chemolithoautotrophs. Among the 895 shared genes
29 were a subset of those hypothesized for Mn(II) oxidation (*Cyc2* and *PCC_1*) and oxygen reduction
30 (*TO_1* and *TO_2*) that could facilitate Mn(II) lithotrophy. An unusual, plausibly reverse Complex
31 1 containing 2 additional pumping subunits was also shared by the family, as were genes for the
32 reverse TCA carbon fixation cycle, which could enable Mn(II) autotrophy. All members of the
33 family lacked genes for nitrification found in *Nitrospira* species. The results suggest that *Ca.*
34 *Manganitrophaceae* share a core set of candidate genes for the newly discovered manganese
35 dependent chemolithoautotrophic lifestyle, and likely have a broad, global distribution.

36

37 **Importance**

38 Manganese (Mn) is an abundant redox-active metal that cycled in many of Earth's biomes. While
39 diverse bacteria and archaea have been demonstrated to respire Mn(III/IV), only recently have
40 bacteria been implicated in Mn(II) oxidation dependent growth. Here, two new Mn(II)-oxidizing
41 enrichment cultures originated from two continents and hemispheres were examined. By
42 comparing the community composition of the enrichments and performing phylogenomic analysis
43 on the abundant *Nitrospirota* therein, new insights are gleaned on cell interactions, taxonomy, and
44 machineries that may underlie Mn(II)-based lithotrophy and autotrophy.

45

46 **Introduction**

47 Members of the bacterial phylum *Nitrospirota* (formerly *Nitrospirae*) are best known for having
48 physiologies that exploit the utilization of high potential electron donors or low potential electron
49 acceptors (1, 2). Cultivated organisms representing this phylum cluster within 4 clades. Order
50 *Nitrospirales* (formerly genus *Nitrospira*) plays an important role in the nitrogen cycle, carrying
51 out nitrite oxidation (3, 4) and complete ammonium oxidation to nitrate (5, 6). Class *Leptospirilla*
52 (formerly genus *Leptospirillum*) thrive in low pH environments oxidizing iron (7). Class
53 *Thermodesulfobacteria* (formerly genus *Thermodesulfobacterium*) includes high temperature
54 dissimilatory sulfate-reducers (8), some with the capacity of S disproportionation (9), as well as
55 uncultivated magnetotactic bacteria (10). Recently, a bacterial co-culture was demonstrated to
56 perform Mn(II) oxidation dependent chemolithoautotrophic growth (11). This metabolism was
57 attributed to a member of a previously uncultivated clade of *Nitrospirota*, *Candidatus*
58 *Manganitrophus noduliformans* strain Mn1, given that the minority member in the co-culture,
59 *Ramlibacter lithotrophicus* (*Comamonadaceae*; formerly within the *Betaproteobacteria*, now
60 within *Gammaproteobacteria*) could be isolated yet would not oxidize Mn(II) alone (11). Based
61 on 16S rRNA gene phylogeny, several relatives of strain Mn1 were identified (11). However,
62 whether or not these relatives might share the same Mn(II) oxidation metabolism was not
63 something that could be gleaned from their rRNA genes.

64
65 Mn is the third most abundant redox-active metal in the Earth's crust and is actively cycled (12–
66 14). Microbial reduction of Mn oxides for growth has been demonstrated in numerous bacterial
67 and archaeal phyla (14–18). The notion that microbial oxidation of Mn(II) with O₂ could serve as
68 the basis for chemolithoautotrophic growth was first theorized decades ago (13, 14, 19, 20). This
69 metabolism, while energetically favorable ($\Delta G^{\circ} = -68$ kJ/mol Mn), poses a biochemical challenge
70 to the cell because of the high average potential of the two Mn(II)-derived electrons
71 (Mn(II)/Mn(IV), $E^{\circ} = +466$ mV (11)). These electrons would need their redox potential to be
72 lowered by nearly a full volt in order to reduce the ferredoxin ($E^{\circ} = -320$ to -398 mV (21))
73 employed in their CO₂ fixation pathway (11). This is a larger and more significant mismatch in
74 redox potential than similar chemolithotrophic metabolisms, such as nitrite or iron oxidation (NO₂⁻
75 /NO₃⁻, $E^{\circ} = +433$ mV (21); Fe(II)/Fe(III), $E^{\circ} \sim 0$ mV (22)). Based on deduced homology with
76 characterized proteins involved with Fe(II) oxidation or aerobic metabolism, genes for 4 putative

77 Mn-oxidizing complexes and 5 terminal oxidases were identified in strain Mn1 and proposed as
78 candidates for energy conservation via electron transport phosphorylation (11). Remarkably, gene
79 clusters for 3 different Complex I exist in strain Mn1 and could facilitate the otherwise endergonic
80 coupling of Mn(II) oxidation to CO₂ reduction, allowing for autotrophic growth via reverse
81 electron transport, i.e. expending motive force to drive down electron reduction potential (11). The
82 apparent redundancy of diverse novel complexes in several members of the family remains
83 puzzling. It seems clear that the identification and analysis of additional strains and genomes of
84 Mn(II)-oxidizing chemolithoautotrophs could likely shed light on the complexes essential for this
85 newfound mode of metabolism.

86

87 The ever increasing number of metagenome-assembled genomes (MAGs) available in the
88 databases provides for an unprecedented opportunity to learn about the gene content and potential
89 functions of many uncultured microorganisms. Yet, cultivation remains critical to forming
90 interconnections between the genomes of both cultured and uncultivated microbes and their
91 metabolisms. Herein, we successfully established new in vitro enrichment cultures performing
92 chemolithoautotrophic Mn oxidation from two disparate environmental inoculum sources. By
93 comparing the MAGs of the most abundant organisms present in these enrichments, also members
94 of the *Nitrospirota*, as well as 66 newly and publicly available MAGs in the databases belonging
95 to Nitrospirota clades with unexamined metabolisms, we gain insight into a core set of candidate
96 genes for facilitating chemolithoautotrophic Mn oxidation, as well as the phylogenetic and
97 geographic distribution of known and putatively Mn-oxidizing *Nitrospirota*.

98

99 **Results**

100 **Reproducible cultivation of Mn-oxidizing chemolithoautotrophs.** *Ca. Manganitrophus*
101 *noduliformans* strain Mn1 was accidentally enriched in tap water (11). Using the defined Mn(II)
102 carbonate medium in this previous study (11), new Mn-oxidizing enrichment cultures were
103 successfully established from two distinct sample sources. One inoculum was material from a Mn
104 oxide containing rock surface near Boetsap, Northern Cape, South Africa (“South Africa
105 enrichment”), and the other inoculum was material from an iron oxide microbial mat in Santa
106 Barbara, California, USA (“Santa Barbara enrichment”). While the new enrichments grew in the
107 same defined freshwater medium, they exhibited different temperature optima. The South Africa
108 enrichments initially grew at 28.5°C, although they oxidized Mn(II) faster at 32°C, similar to the
109 previous enrichment from the Pasadena drinking water distribution system (“Pasadena
110 enrichment”) (11). The Santa Barbara enrichments grew at 28.5°C, but not at 32°C. Otherwise, no
111 striking differences in appearance (e.g. formation of small Mn oxide nodular products) between
112 the three cultures was observed. These results indicate that the defined Mn(II) carbonate medium
113 can successfully be employed during intentional, directed attempts to cultivate Mn-oxidizing
114 chemolithoautotrophs from diverse terrestrial and aquatic freshwater environments.

115
116 **Community analysis of Mn-oxidizing enrichment cultures from three origins.** As was the case
117 with cultures of *Ca. M. noduliformans*, repeated attempts to identify single colonies of the
118 lithotrophs responsible for Mn oxidation were not successful on an agar-solidified, defined Mn(II)
119 carbonate medium. Sequencing of partial 16S rRNA genes amplified from the liquid cultures
120 revealed differences in community structures between the Mn-oxidizing enrichments. The most
121 abundant microorganism from the South Africa and Santa Barbara enrichments belonged to the
122 same taxon as the previously described *Ca. M. noduliformans* (Figure 1). However, the identities
123 of the next most abundant members of the communities differed. The previously described
124 Pasadena enrichment containing *Ca. M. noduliformans* had *Ramlibacter lithotrophicus* as the
125 second most abundant member throughout the enrichment refining process (Supplementary Table
126 1). *R. lithotrophicus* could be isolated from the enrichment using the same defined medium but
127 with other electron donors such as succinate and hydrogen, but could not oxidize Mn(II) as an
128 isolate (11). Organisms belonging to the same taxon as *R. lithotrophicus* were present in the South
129 Africa enrichments, varying from 2-28 in rank abundance, but were not abundant in Santa Barbara

130 enrichments (<0.5% relative abundance) (Figure 1 and Supplementary Table 1). In the South
131 Africa enrichments, the second most abundant member varied between a *Pseudomonas* species
132 (*Gammaproteobacteria*), a member of the *Zavarziniales* (*Alphaproteobacteria*), *R. lithotrophicus*,
133 and *Hydrogenophaga* (a *Comamonadaceae* closely related to *R. lithotrophicus*) (Figure 1). In the
134 Santa Barbara enrichments, the second most abundant member was a member of the
135 *Anaerolineaceae* (phylum *Chloroflexi* or *Chloroflexota*; Figure 1). Changing the incubation
136 temperature did not affect the identities of the 3 most abundant taxa in the South Africa
137 enrichments (Figure 1). However, the choice of nitrogen source in the medium resulted in a shift
138 in community member relative abundances (Figure 1). Notably, the only other shared organism
139 between South Africa, Santa Barbara and Pasadena enrichments with >1% relative abundance was
140 a member of the *Zavarziniales* (Figure 1 and Supplementary Table 1). Its relative abundance
141 markedly increased when the South Africa enrichments were grown in medium with nitrate instead
142 of ammonia as the nitrogen source. Overall, while the community composition varied between the
143 Mn-oxidizing enrichments, strains of *Ca. Manganitrophus* were consistently the most abundant
144 species in all such cultures.

145
146 **Expansion of metagenome-assembled genomes of cultivated and environmental Mn-**
147 **oxidizing *Nitrospirota*.** We performed shotgun metagenomic sequencing on two of the new Mn-
148 oxidizing enrichments in order to gain phylogenetic and functional insights into the newly
149 cultivated *Ca. Manganitrophus* strains. We reconstructed high-quality MAGs (>97%
150 completeness, <5% contamination) (23) of the most abundant organism from each metagenome
151 (Supplementary Table 1). We refer to these MAGs as strain SA1 and SB1 to indicate that they
152 originated from South Africa and Santa Barbara, respectively. Both genome and 16S rRNA gene
153 phylogenies confirmed that strain SA1 and strain SB1 were related to the previously characterized
154 *Ca. M. noduliformans* strain Mn1 (Figure 2). Based on their average nucleotide identities (ANI)
155 and using 95% ANI as a possible metric for species delineation (24–26), strains SA1 and SB1 were
156 provisionally considered to represent distinct strains of the same species (96% ANI). Both could
157 be considered a different species than strain Mn1 (94% ANI) (Supplementary Table 3). The
158 genome sizes of these 2 new strains were smaller (4.3 Mb) than that of strain Mn1 (5.2 Mb)
159 (Supplementary Table 2). The arrangement of homologous regions in strains SA1 and SB1 were
160 similar (Supplementary Figure 1a), but were different from strain Mn1 (Supplementary Figure 1b).

161 These differences were also observed at the deduced protein level, with strains SA1 and SB1 more
162 closely related to each other than to strain Mn1 (Supplementary Table 4). These variations in the
163 proteins were not concentrated in one genomic region, but instead scattered throughout the genome
164 (Supplementary Figure 1c). Further, de novo gene clustering showed that strains SA1 and SB1
165 shared more genes with each other than with strain Mn1 (Supplementary Figure 1d). All together,
166 our results support strains SA1 and SB1 as a distinct species, which we designate as *Candidatus*
167 *Manganitrophus morganii* (Supplementary Text). These 3 cultivated *Ca. Manganitrophus* strains
168 in two different species provide a basis to examine the phylogenetic and genomic diversity of their
169 shared metabolism, namely Mn-oxidizing chemolithoautotrophy.

170
171 In addition to reconstructing MAGs from Mn-oxidizing enrichments, we also analyzed publicly
172 available MAGs in the phylum *Nitrospirota*. We screened for MAGs that did not belong in the
173 three characterized clades, namely *Nitrospirales*, *Leptospirilla* and *Thermodesulfovibria*. As of 26
174 March 2019, only 3 MAGs had met this taxonomic criteria with completeness >50% and
175 contamination <5% (11). However, as of March 30 2021, 64 new public high-quality (>90%
176 completeness, <5% contamination) and 2 medium-quality (>50% completeness, <10%
177 contamination) MAGs meeting this taxonomic criteria had become available (Supplementary
178 Table 5). These 66 MAGs allowed for a much more detailed phylogenomic view into the
179 uncultivated *Nitrospirota* and their potential ability to oxidize Mn.

180
181 **16S rRNA gene and multilocus protein phylogeny reveal robust taxonomic groups.** The
182 available MAGs provide a phylogenetic resolution that matches the traditionally employed 16S
183 rRNA genes (Figure 2). The MAGs were spread out across different phylogenetic clusters within
184 the phylum (Figure 2a). Using the 14 MAGs that also contained 16S rRNA genes, we were able
185 to link the genome phylogeny to the 16S rRNA gene phylogeny, and observed similar clusterings
186 between the two phylogenetic approaches (Figure 2). The 3 cultivated strains all resided within
187 the genus *Ca. Manganitrophus*. Other members of *Ca. Manganitrophus*, based on either their
188 genomes or 16S rRNA genes, were from terrestrial, aquatic and engineered environments, and all
189 freshwater in origin (Figure 2). Our phylogeny revealed a sister genus of marine origin (Figure 2).
190 Together, these two genera form a coherent and well supported phylogenetic clade, hereafter
191 termed family *Candidatus Manganitrophaceae* (Figure 2).

192
193 Previously, the class *Candidatus* Troglögloea was proposed to encompass strain Mn1 and
194 *Candidatus* Troglögloea absoloni (an uncultivated species from Vjetrenica cave in the Dinaric
195 Karst), based on their 16S rRNA gene phylogeny (11). Based on our new phylogenomic analysis,
196 we propose that the order *Ca.* Troglögloeales includes the family *Ca.* Manganitrophaceae, *Ca.* T.
197 absoloni, and its relatives (Figure 2), together constituting a sister group distinct from the order
198 *Nitrospirales* (which includes the cultivated nitrite and ammonia-oxidizing *Nitrospirota*). These
199 genera, family, and order proposals are consistent with the latest taxonomic classification in the
200 Genome Taxonomy Database (GTDB) release 06-RS202 April 2021 (27, 28), even though GTDB
201 currently contains fewer genomes. Based on the current GTDB taxonomy, both orders *Ca.*
202 Troglögloeales and *Nitrospirales* are placed within the class *Nitrospiria*, but this is incongruent
203 with analyses of their 16S rRNA phylogeny (Figure 2b). Numerous *Nitrospirota* MAGs fall
204 outside of the three known groups of *Nitrospirota* (*Nitrospirales*, *Leptosprillia* and
205 *Thermodesulfobibriona*) and are over-represented in subsurface and aquatic environments.
206 However, 16S rRNA gene surveys indicate that members of many of the uncultivated clades exist
207 from marine, soil and sediment environments, but are not as of yet represented by genomes (Figure
208 2b). Overall, while the taxonomic relationship between orders *Ca.* Troglögloeales and
209 *Nitrospirales* and the assignment of classes in *Nitrospirota* remains to be resolved, our proposals
210 of the genus *Ca.* Manganitrophus, family *Ca.* Manganitrophaceae, and order *Ca.* Troglögloeales
211 are supported by both 16S rRNA gene and genome phylogenetic approaches, and additionally
212 reveal members of a novel marine genus that possibly oxidize Mn lithotrophically.

213
214 **Genome comparison streamlines the hypothesized genes for Mn-oxidizing lithotrophy.** We
215 next compared the MAGs of members of the family *Ca.* Manganitrophaceae to understand which
216 genes might be candidates as essential for Mn oxidation, and whether these are found in
217 representatives of the marine genus or other members in the phylum. Four routes for Mn oxidation
218 and electron uptake had been previously hypothesized in strain Mn1, including a Cyc2 and three
219 different porin-dodecaheme cytochrome *c* (PCC) complexes (11). Cyc2 homologs are not only
220 identified in the majority of *Ca.* Troglögloeales (Figure 3a), but also in other members of the
221 phylum, including characterized clades such as acidophilic, iron-oxidizing *Leptosprillia* and nitrite
222 or ammonia-oxidizing *Nitrospirales* (29, 30). Of the 3 PCCs in strain Mn1, only PCC_1 was found

223 in the strains SA1 and SB1 (Figure 3a). PCC_1 was also identified in other MAGs in both marine
224 and freshwater genera of *Ca. Manganitrophaceae*, but not in the extant MAGs and genomes of
225 *Nitrospirota* species falling out outside of this family. These results point to PCC_1, possibly
226 together with Cyc2, as being central to chemolithotrophic Mn oxidation by *Ca.*
227 *Manganitrophaceae*.

228
229 We identified five possible routes in strain Mn1 to reduce oxygen and conserve energy using
230 electrons from Mn(II). The canonical Complex IV (*cbb3*-type cytochrome *c* oxidase) was
231 identified in the cultivated and uncultivated members of the freshwater genus, but not in the
232 uncultivated members of the marine genus (Figure 3a). However, the expression of this Complex
233 IV had been observed to be low (24th percentile) in strain Mn1, especially so for a catabolic
234 process, and therefore may not be the primary route for oxygen respiration (11). Genes for a
235 canonical cytochrome *bd* oxidase, which has been hypothesized to reduce oxygen in *Leptospirilla*
236 (31), were not found in strain Mn1 or other members in the order *Ca. Trogloloeales* (Figure 3a).
237 However, genes for a number of cytochrome *bd* oxidase-like (*bd*-like) proteins that were
238 phylogenetically distinct and predicted to have many more transmembrane helices than
239 cytochrome *bd* oxidase (32), were identified in strain Mn1 (11). These *bd*-like oxidases are
240 clustered with other genes potentially involved in electron transfer and energy conservation; we
241 refer to these *bd*-like oxidase containing gene clusters as terminal oxidase (TO) complexes. While
242 all 4 TO complexes were found in other members of *Ca. Trogloloeales*, their taxonomic
243 distributions differed (Figure 3a). TO_1 was found in the majority of *Ca. Trogloloeales* (Figure
244 3a), and have been well discussed in other *Nitrospirota* including *Nitrospirales* (32, 33). TO_1 is
245 composed of a *bd*-like oxidase clade I protein, two cytochrome *c* and a periplasmic cytochrome *b*,
246 and was the highest expressed TO complex (98th percentile) in strain Mn1 (11). Contrasting with
247 the more widespread distribution of the TO_1 complex across the phylum, complexes TO_2, TO_3
248 and TO_4 were restricted to *Ca. Manganitrophaceae*, with the latter two limited to the freshwater
249 genus (Figure 3a). While both TO_3 and TO_4 contain two *bd*-like oxidase clade V proteins, their
250 predicted interactions with the quinol pool differ: TO_3 encodes for an Alternative Complex III,
251 whereas TO_4 encodes for a more canonical Complex III (11). TO_3 and TO_4 were observed to
252 be moderately expressed at 55th and 67th percentile in strain Mn1, respectively (11). Importantly,
253 TO_2 stands out as it was found in the majority of *Ca. Manganitrophaceae*, but as yet to be

254 identified in any genomes outside of this family (Figure 3a). The TO_2 gene arrangement differed
255 slightly between the two genera of *Ca. Manganitrophaceae*, but gene content was similar (Figure
256 3c). The TO_2 complex is composed of a membrane cytochrome *b* (similar to the petB/D or
257 cytochrome *bf* complex) and potentially interacts with the quinone pool, a periplasmic cytochrome
258 *b* to receive electrons in the periplasm, *bd*-like oxidase to reduce oxygen, multiple cytochrome *c*
259 to transfer electrons, and two ion-pumping *mrpD*-like subunits that might be coupled to the
260 generation or dissipation of a motive force (Figure 3c). Genes for the TO_2 complex had also been
261 observed to be highly expressed in strain Mn1 (79th percentile) (11). Taken together, our
262 comparative genomic analyses point to TO_2, possibly together with TO_1, as being central to
263 Mn(II)-oxidation-dependent oxygen respiration by *Ca. Manganitrophaceae*.

264
265 **Autotrophic pathway predicted in Mn-oxidizing *Nitrospirota*.** In addition to coupling the
266 oxidation of Mn(II) to oxygen reduction, strain Mn1 was also shown to be capable of CO₂ fixation
267 and autotrophic growth using Mn(II) as its electron donor (11). Carbon fixation pathways such as
268 the reverse tricarboxylic acid (rTCA) cycle, implicated in autotrophy by strain Mn1, require low
269 potential electrons in the form of both NAD(P)H and ferredoxin ($E^{\circ'} = -320$ to -398 mV (21))
270 (34). Yet, electrons derived from Mn(II) are likely high potential ($E^{\circ'} = +466$ mV) (11, 12). Run
271 in reverse, Complex I has been shown or postulated to couple the dissipation of motive force to
272 the generation of low potential electrons and production of NAD(P)H or possibly ferredoxin (11,
273 35, 36).

274
275 Remarkably, in strain Mn1, 3 different Complex I gene clusters were previously identified (11).
276 Complex_I_1 and Complex_I_2 are similar to canonical Complex I with gene clusters containing
277 *nuoA-N* genes in order (Supplementary Figure 2). Here, phylogenomic analyses revealed that
278 Complex_I_1 was shared by all members of both genera of *Ca. Manganitrophaceae*, whereas
279 Complex_I_2 was restricted to members of the freshwater genus (Figure 3a). Of note,
280 Complex_I_3 appears unique in the known biological world, having two additional ion-pumping
281 subunits (Figure 4). This highly unusual gene cluster was found in nearly all of *Ca.*
282 *Manganitrophaceae* (Figure 3a) and is not apparent in any other member of the phylum. Unusual
283 Complex I with one additional ion-pumping subunit have been previously observed in various
284 bacterial groups including *Nitrospirales*, termed 2M Complex I given the extra *nuoM* in the gene

285 cluster (35), and rhizobia, termed Green Complex I in which 2 *mrpD*-like subunits have replaced
286 the standard *nuoL* (37). Sequence comparison of Complex_I_3 subunits showed that the two
287 MrpD-like subunits were most closely related to those in rhizobia Green Complex I, while the
288 other subunits in the gene cluster were most closely related to those in *Nitrospira* 2M Complex I
289 (Figure 4a). Sequence alignment of MrpD2 revealed a 26 amino acid insertion in the C-terminal
290 amphipathic helix (HL) in all of *Ca. Manganitrophaceae* as compared to the MrpD subunits found
291 in the rhizobia Green Complex I (Figure 4b). This type of insertion was previously identified in
292 all gene clusters containing a second ion-pumping subunit (35). Such insertions were not unique
293 to Complex_I_3, as they were also found in the NuoL of Complex_I_1 and Complex_I_2 in *Ca.*
294 *Manganitrophaceae* (Supplementary Figure 2) and could represent evolutionary intermediates en
295 route to being able to support additional ion-pumping subunits in the protein complex (Figure 4c).
296

297 The majority of *Ca. Trogloloeales* and all of *Ca. Manganitrophaceae* analyzed had complete sets
298 of genes for the rTCA cycle (Figure 3a). Only a minor difference was observed in the rTCA cycle
299 gene content: members of the freshwater genus contained class II fumarate hydratase, whereas
300 those of the marine genus contained class I fumarate hydratase. To further assimilate pyruvate,
301 nearly all genes of the gluconeogenic pathway (Embden-Meyerhof-Parnas pathway) were
302 observed in *Ca. Trogloloeales*. However, one key gluconeogenic pathway gene, namely fructose-
303 biphosphate aldolase, was absent in strain Mn1 (11) and also appears absent from the majority of
304 *Ca. Trogloloeales*, save for except two of the MAGs (NCBI assembly accession:
305 GCA_004297235 and GCA_013151935). Moreover, our comparative analysis revealed that only
306 1 of the 5 pyruvate dehydrogenases encoded by the genome of strain Mn1 (IMG gene ID:
307 Ga0306812_1021045-Ga0306812_1021047, Ga0306812_102629) was common to the other
308 members of the *Ca. Manganitrophaceae*. Overall, despite apparently minor differences between
309 their MAGs, the majority of *Ca. Manganitrophaceae* shared the same unique Complex_I_3,
310 pathways for CO₂ fixation and pathways for central metabolism as had been previously identified
311 in strain Mn1.

312

313 **Core genome of *Ca. Manganitrophaceae* in marine and freshwater environments.** De novo
314 gene clustering revealed that 8 analyzed members of *Ca. Manganitrophaceae* shared a total of 895
315 gene clusters, which included the above-mentioned Cyc2, PCC_1, TO_1, TO_2, Complex_I_1

316 and Complex_I_3 (Supplementary Table 6). Several other shared genes and pathways appear
317 noteworthy: assimilatory sulfate reduction (*sat*, *aprA/B*, *aSir*), cytochrome *c* biogenesis, heme
318 exporters, 2 multicopper oxidases, and type IV pilus assembly. These confirm the basis for the
319 ability of the cultivated strains to use sulfate as an anabolic sulfur source, make cytochrome *c* for
320 anabolism and catabolism, and suggest the potential for surface twitching motility. Notably
321 missing among the shared genes were those for the carbon-monoxide dehydrogenase complex that
322 had been observed to be highly expressed (95th percentile) during Mn(II) dependent growth by
323 strain Mn1 (11). Together, our comparative genomic analyses shed light on common gene sets of
324 Mn-oxidizing chemolithoautotrophs in both marine and freshwater environments.

325

326

327 **Discussion**

328 Cultivation of novel microorganisms with previously undemonstrated physiologies remains a key
329 cornerstone to our expanding understanding of the metabolic potential of the as yet largely
330 uncultured microbial diversity in nature (38, 39). Aerobic, Mn(II)-oxidizing chemolithoautotrophs
331 were long theorized, but only recently demonstrated to exist in vitro in a bacterial co-culture (11).
332 The majority member was a distinct member of the phylum *Nitrospirota*, *Ca. Manganitrophus*
333 noduliformans strain Mn1, and only distantly related to any other cultivated biota (11). Curiously,
334 the initial enrichment of Mn(II)-oxidizing chemolithoautotrophs from Caltech's campus tap was
335 unintentional (11). Here cultivation attempts were intentionally initiated with the specific goal of
336 successfully establishing new Mn-oxidizing enrichment cultures. These attempts were successful
337 using a media formulation refined during the course of the earlier study using inocula obtained
338 from two different continents and hemispheres. Community analyses on these two new enrichment
339 cultures revealed that the most abundant microorganisms in each were closely related to, but of a
340 different species than *Ca. M. noduliformans* strain Mn1. The enrichment cultures also harbored a
341 diversity of taxa varying in their relative abundances and identities (Figure 1). The results support
342 the notion that members of the genus *Ca. Manganitrophus* are playing a key if not the central role
343 in chemolithoautotrophic Mn(II) oxidation in the laboratory cultures examined. The results also
344 suggest that *Ca. Manganitrophus* may not require an obligate partnership with *R. lithotrophicus*
345 (the second species present in the previously described co-culture (11)), leaving open the
346 possibility that its eventual clonal isolation may be possible. The phylogenomic analyses here also
347 predict an assemblage of a marine genus within the family *Ca. Manganitrophaceae* that may also
348 carry out this mode of chemolithoautotrophy (Figure 2, 3, and 4). However, our analyses do not
349 exclude other members in *Nitrospirota* carrying out Mn(II) lithotrophy using a different
350 mechanism than that we hypothesized for *Ca. Manganitrophaceae*. With the increasing evidence
351 that the *Ca. Manganitrophaceae* are distributed globally across marine and freshwater biomes
352 (Figure 5a), taken together the reported prevalence of Mn and Mn-reducing microorganisms in the
353 environment (14, 40), chemolithoautotrophic Mn oxidation becomes particularly important to
354 reaching a better understanding of the redox biogeochemical cycle for manganese.

355

356 By comparing metagenome-assembled genomes of the 3 cultivated *Ca. Manganitrophus* strains
357 and related but uncultivated organisms available in public genome databases, our results narrow

358 down the list of genes in *Ca. Manganitrophaceae* that may underlie Mn(II) oxidation driven
359 chemolithoautotrophy. Unique to *Ca. Manganitrophaceae* among all *Nitrospirota*, and perhaps
360 across all of the biological world that has yet been analyzed, were PCC_1, as a candidate for being
361 the initial electron acceptor during Mn oxidation; TO_2, as a candidate respiratory complex for
362 productively coupling the electrons from Mn(II) oxidation to oxygen reduction and energy
363 conservation (Figure 3 and Figure 5b); and Complex_I_3, as a candidate complex catalyzing
364 reverse electron transport to generate low-potential reducing power from quinones during carbon
365 fixation (Figure 4, Figure 5b).

366
367 While not unique to *Ca. Manganitrophaceae*, the identification of Cyc2 and TO_1 in the majority
368 of the family members (Figure 3a and 4b), together with their comparable or even higher
369 expression than that of PCC_1 and TO_2, respectively, in strain Mn1 (11), suggests that these two
370 complexes may also be likely involved in Mn lithotrophy. Cyc2 is a fused cytochrome-porin
371 protein with a single heme *c*, whereas porin cytochrome *c* (PCC) are larger complexes composed
372 of a beta-barrel outer membrane protein and at least one multiheme cytochrome *c* (41–43). Best
373 understood in acidophilic and circum neutral pH Fe(II) oxidation, predicted structural differences
374 between Cyc2 and PCC homologs, specifically the smaller porin size of Cyc2 and the inner
375 placement of heme *c* within the porin, have been suggested as meaning that Cyc2 may only react
376 with dissolved Fe²⁺ species (29), whereas PCC homologs might react with both soluble and
377 insoluble forms of Fe(II). In the case of Mn(II) oxidation, the reaction is thought most likely to
378 proceed via two sequential one-electron oxidation steps (44). In that case, Cyc2 and PCC_1 might
379 react with different forms or oxidation states of Mn (e.g. Mn(H₂O)₆²⁺ vs MnCO₃, Mn(II) vs Mn(III)
380 complexes) that have different solubilities. In comparison, known heterotrophs that catalyze
381 Mn(II) oxidation often employ multicopper oxidase (MCO) or heme peroxidase homologs to
382 oxidise this metal (45–47). However, the nature of these enzymes is to couple the oxidation of Mn
383 to the direct reduction of oxygen, without a clear path for conserving any of the potential free
384 energy energy for use by the cell. Members of *Ca. Manganitrophaceae* encodes two MCOs each
385 (Supplementary Table 6). It is possible that these too could be involved in the lithotrophic
386 oxidation of Mn(II); if so, it seems likely that the MCO would transfer Mn(II)-derived electrons
387 to a periplasmic electron carriers such as cytochrome *c*, rather than directly to molecular oxygen,
388 to be able to conserve energy for the cell (48).

389

390 Instead of the canonical cytochrome *c* oxidase common to many aerobes, *Ca. Manganitrophaceae*
391 likely use poorly characterized terminal oxidase (TO) complexes for oxygen respiration (Figure
392 5b). In strain Mn1, 4 TO complexes that contain *bd*-like oxidases to reduce oxygen were identified,
393 but the genes for the other components of these complexes differed between them, and likely
394 distinguish their cellular functions (11). TO_1 contained a CISM periplasmic cytochrome *b* that
395 may receive electrons from the periplasm, whereas TO_3 and TO_4 contained Complex III or
396 Alternative Complex III like components that may interact with the quinone pool (11). TO_2
397 stands out, not only because it was found to be unique to the *Ca. Manganitrophaceae*, but also
398 because it contains a periplasmic and a membrane cytochrome *b* that might both receive electrons
399 from the periplasm and engage in electron transfer with the quinone pool (Figure 3c and 4b). In
400 theory, there may be a scenario in which TO_2 bifurcates Mn(II)-derived electrons ($E^{\circ'} = +466$
401 mV) to reduce oxygen ($E^{\circ'} = +818$ mV, via its *bd*-like oxidase) and quinones ($E^{\circ'} \sim +113$ mV, via
402 its membrane cytochrome *b*), while using its 2 MrpD like ion-pumping subunits, unusual
403 components of a terminal oxidase, to dissipate a membrane motive force and drive the endergonic
404 reduction of quinones (Figure 5b).

405

406 Unusual arrangements of Complex I involving additional ion-pumping subunits may be relevant
407 to the process of generating low-potential reducing power from quinones (35). Our analyses of
408 Complex_I_3 examining subunit similarities, gene clustering, and the presence of specific
409 insertions (Figure 4a and 4b) suggest an evolutionary hybridization wherein the MrpD subunits of
410 a rhizobia-like Green Complex I replaced the NuoL of a *Nitrospira*-like 2M Complex I, with an
411 additional HL extension needed in MrpD2 of Complex_I_3 to accommodate the second NuoM
412 (Figure 4c). If run in reverse, this highly unusual complex, having a total of 5 ion-pumping
413 subunits, might serve to transfer electrons from the reduced quinone pool to a carrier having a
414 lower reduction potential than that of NADH, such as a ferredoxin required for the rTCA cycle
415 (Figure 5b). That is, the complex could serve to dissipate the motive force built up during Mn(II)
416 lithotrophy, by coupling the inward flow of 6 protons or sodium ions with the endergonic reduction
417 of a ferredoxin using a quinol (Figure 4c and 5b). The additional pumping subunit would be
418 necessary in *Ca. Manganitrophaceae* as compared to *Nitrospira* species, which have similar

419 reverse electron transfer requirements when using high potential electron donors such as nitrite or
420 ammonia, but are of moderately lower potential than Mn(II) derived electrons.

421

422 Based on our phylogenomic analyses, a set of shared, unique complexes in *Ca.*
423 Manganitrophaceae, namely PCC_1, TO_2 and Complex_I_3, become prime targets for future
424 physiological and biochemical examination, in efforts to better understand the cellular machinery
425 enabling Mn(II)-dependent chemolithoautotrophy. Much of our proposed routes of Mn(II)
426 oxidation are in large part informed by our existing knowledge on Fe(II) oxidation. Fe(II) oxidizers
427 have been found in diverse marine and freshwater environments (49, 50), as is now the case for
428 cultivated and demonstrated, as well as uncultivated and putative Mn(II) oxidizers in *Ca.*
429 Manganitrophaceae (Figure 5a). Taxonomically, Fe(II) oxidizers have been identified in several
430 phyla of bacteria and archaea (49, 50) and can be acidophiles or neutrophiles, mesophiles or
431 thermophiles, phototrophs or chemotrophs, heterotrophs or autotrophs, and aerobes or anaerobes
432 (49, 50). If such extends to the biology of energetic Mn(II) oxidation, the results gleaned here from
433 the cultivation and phylogenomics of *Ca.* Manganitrophaceae may be only the first glimpse into
434 the full diversity of microorganisms capable of coupling Mn(II) oxidation to growth.

435

436 **Material and Methods**

437 Cultivation

438 The enrichment procedure and manganese carbonate media composition (using 1 mM nitrate or
439 ammonia as the N source, as noted) were described previously (11). Unless stated otherwise,
440 culturing was performed in 10 ml of medium in 18-mm culture tubes. Cultures were transferred
441 (10% v/v) when laboratory prepared MnCO₃ (light pink or tan color) were completely converted
442 to Mn oxide (dark or black color).

443

444 The South Africa inoculum was collected in June 2017 from a rock surface near a pond by a road
445 on an exposed outcrop of the Reivilo Formation (lat. -27.964167, long. 24.454183, elevation 1107
446 m) near Boetsap, Northern Cape, South Africa. The rock was coated with a black material, of a
447 texture between slime and moss. A thin, laminated green mat was observed underlying the black
448 material. The black material reacted to leucoberbelin blue dye, indicating the presence of
449 manganese oxides. A mixture of the black and green material was sampled using an ethanol-
450 sterilized spatula into a sterile 15-ml tube and stored at room temperature until inoculation. The
451 cultures were initiated in medium with 1 mM ammonia and incubated at 28.5°C. Later, some were
452 transferred to medium with 1 mM nitrate and/or incubated at 32°C.

453

454 The Santa Barbara inoculum was collected in November 2018 from an iron oxide mat surrounded
455 by reeds at the outflow of a rusted iron pipe (lat. 34.417944, long. -119.741130) along the side of
456 a road in Santa Barbara, California, USA. The iron oxide mat was fluffy with a typical dark orange
457 color. The mat was collected in a glass jar and stored at room temperature until inoculation. The
458 enrichment cultures were incubated at 28.5°C and later some were transferred to incubate 32°C,
459 all in the basal MnCO₃ medium with 1 mM nitrate. The initial enrichment was transferred 5 times
460 to confirm Mn-oxidizing activity and refine community composition prior to community and
461 metagenomic analysis.

462

463 Community analysis using 16S rRNA gene amplicon sequencing

464 Mn oxides were harvested from stationary phase enrichment cultures: 2 ml of culture containing
465 ca. 0.15 g of Mn oxide nodules was sampled into a 2-ml Eppendorf tube and centrifuged at 8000
466 × g for 3 min at room temperature. After carefully removing the supernatant by pipetting, DNA

467 was immediately extracted from the pellets using the DNeasy PowerSoil kit (Qiagen, Valencia,
468 CA, USA) following the manufacturer's instructions, with the bead beating option using FastPrep
469 FP120 (Thermo Electron Corporation, Milford, MA, USA) at setting 5.5 for 45 s instead of the 10
470 min vortex step. DNA concentration was quantified using Qubit dsDNA High Sensitivity Assay
471 Kit (Thermo Fisher Scientific, Waltham, MA, USA).

472

473 For 16S rRNA gene amplicon sequencing, the V4-V5 region of the 16S rRNA gene was
474 amplified from the DNA extracts using archaeal/bacterial primers with Illumina (San Diego, CA,
475 USA) adapters on 5' end (515F 5'-
476 TCGTCGGCAGCGTCAGATGTGTATAAGAGACAGGTGYCAGCMGCCGCGGTAA-3' and
477 926R 5'-GTCTCGTGGGCTCGGAGATGTGTATAAGAGACAG-
478 CCGYCAATTYMTTTRAGTTT-3'). Duplicate PCR reactions were pooled, barcoded, purified,
479 quantified and sequenced on Illumina's MiSeq platform with 250 bp paired end sequencing as
480 previously described (11). Raw reads with >1 bp mismatch to the expected barcodes were
481 discarded, and indexes and adapters were removed using MiSeq Recorder software (Illumina).
482 Then, the reads were processed using QIIME2 release 2020.11 (51). Briefly, forward and reverse
483 reads were denoised using DADA2 (52) by truncating at positions 200 and 240, respectively,
484 leaving 28 bp overlaps. Read pairs were merged, dereplicated and chimera removed with the
485 "pooled" setting using DADA2 (52). Taxonomic assignments for the resulting amplicon
486 sequencing variants (ASVs) used a pre-trained naive Bayes classifier on the full-length 16S
487 rRNA genes in SILVA 138 SSURef NR99 database (53, 54). ASVs assigned to the same level 7
488 taxonomy were combined, and those assigned to mitochondria, chloroplast, or without taxonomy
489 assignments were removed using the --p-exclude
490 mitochondria,chloroplast,"Bacteria;Other;Other;Other;Other;Other;Other","Unassigned;Other;Other;Ot
491 her;Other;Other" setting.

492

493 Metagenomics

494 Purified genomic DNA samples (2-50 ng) were fragmented to the average size of 600 bp via use
495 of a Qsonica Q800R sonicator (power: 20%; pulse: 15 sec on/15 sec off; sonication time: 3 min).
496 Libraries were constructed using the NEBNext Ultra™ II DNA Library Prep Kit (New England

497 Biolabs, Ipswich, MA) following the manufacturer's instructions by Novogene Corporation Inc
498 (Sacramento, CA, USA). Briefly, fragmented DNA was end-repaired by incubating the samples
499 with an enzyme cocktail for 30 mins at 20 °C followed by a second incubation for 30 mins at
500 65 °C. During end repair, the 5' end of the DNA fragments are phosphorylated and a 3' 'A' base is
501 added through treatment with Klenow fragment (3' to 5' exo minus) and dATP. The protruding 3'
502 'A' base was then used for ligation with the NEBNext Multiplex Oligos for Illumina (New England
503 Biolabs) which have a single 3' overhanging 'T' base and a hairpin structure. Following ligation,
504 adapters were converted to the 'Y' shape by treating with USER enzyme and DNA fragments were
505 size selected using Agencourt AMPure XP beads (Beckman Coulter, Indianapolis, IN, USA) to
506 generate fragment sizes between 500 and 700 bp. Adaptor-ligated DNA was PCR amplified with
507 9 to 12 cycles depending on the input amount followed by AMPure XP bead clean up. Libraries
508 were quantified with Qubit dsDNA HS Kit (Thermo Fisher Scientific) and the size distribution
509 was confirmed with High Sensitivity DNA TapeStation assay (Agilent Technologies, Santa Clara,
510 CA, USA). Sequencing was performed on the HiSeq platform (Illumina) with paired 150 bp reads
511 following manufacturer's instructions (Novogene). Base calls were performed with RTA v1.18.64
512 followed by conversion to FASTQ with bcl2fastq v1.8.4 (Illumina). In addition, reads that did not
513 pass the Illumina chastity filter as identified by the Y flag in their fastq headers were discarded.

514
515 The resulting reads were uploaded to the KBase platform (55), trimmed using Trimmomatic v0.36
516 (56) with default settings and adaptor clipping profile Truseq3-PE, and assembled using Spades
517 v3.11.1 (57) with default settings for standard dataset. Manual binning and scaffolding were
518 performed using mmgenome v0.7.179 based on differential coverage and GC content of different
519 metagenomes to generate the MAG for the most abundant organism. MAGs were annotated using
520 the Rapid Annotations using Subsystems Technology (RAST) (58–60) and NCBI Prokaryotic
521 Genome Annotation (61) Pipelines. Average nucleotide identities and reciprocal mapping of
522 MAGs were done using fastANI v1.32 (24). Average amino acid identities were done using enve-
523 omics tool AAI calculator (26). De novo gene clustering was done using anvio v7 with default
524 parameters (62). Comparison of Complex I gene clusters was done using protein-protein BLAST
525 with default parameters (63) to the RefSeq Select proteins database (64). Alignment of Complex I
526 gene sequences was done using MUSCLE v3.8.1551 with default parameters (65).

527

528 Phylogenetic analyses

529 For genome phylogeny, 433 publicly available genome assemblies in the NCBI Assembly
530 Database (61) fell within the phylum *Nitrospirae* (Taxonomy ID 40117) (66) and 6 publicly
531 available genomes in the genomic catalog of Earth's microbiomes dataset (67) fell within the
532 phylum *Nitrospirota* under the headings Nitrospirota and Nitrospirota_A (27) and were analysed
533 (as of March 30, 2021). For 16S rRNA gene phylogeny, 16s rRNA genes from the MAGs of
534 Nitrospirota from the enrichment metagenomes, as well as the genome assemblies were retrieved
535 using CheckM v1.1.2 (68) ssu_finder utility. Sequences less than 900 bp were excluded. The 16S
536 rRNA gene sequences were aligned using SINA v1.2.11 (69) and imported into SILVA Ref
537 Database Release 138.1 (53). 104 16S rRNA gene sequences, including 5 different outgroup
538 sequences (*Desulfovibrio vulgaris*, *Ramlibacter tataouinensis TTB310*, *Nitrospina gracilis 3/211*,
539 *Acidobacterium capsulatum*, *Candidatus Methyloimabilis oxyfera*), with 1508 nucleotide
540 positions were exported with bacteria filter excluding columns with mostly gaps from the ARB
541 software v6.0.2 (70). Bayesian phylogenetic trees were constructed using MrBayes v3.2.7 (71)
542 with evolutionary model set to GTR + I + gamma, burn-in set to 25% and stop value set to 0.01,
543 and edited in iTOL v6 (72). For concatenated multilocus protein phylogeny, marker proteins from
544 104 genomes including the same 5 outgroup species were identified and aligned using a set of 120
545 ubiquitous single-copy bacterial proteins in GTDB v0.2.2 (27). The protein alignment was filtered
546 using default parameters in GTDB v0.2.2 (27) (the full alignment of 34744 columns from 120
547 protein markers were evenly subsampled with a maximum of 42 columns retained per protein; a
548 column was retained only when the column was in at least 50% of the sequences, and contained at
549 least 25% and at most 95% of one amino acid). The resulting alignment with 5040 amino acid
550 positions was used to construct the multilocus protein phylogeny using MrBayes v3.2.7 (71) as
551 above except the evolutionary model was set to invgamma and a mixed amino acid model.

552

553 Data Availability

554 The partial 16S rRNA gene amplicon sequences of enrichment cultures, and metagenome-
555 assembled genomes of *Candidatus Manganirophus morganii* strains SA1 and SB1 have been
556 deposited in National Center for Biotechnology Information (NCBI) under BioProject
557 PRJNA776098.

558 **Acknowledgements**

559 We thank Stephanie Connon for assistance with 16S rRNA gene amplicon sequencing and
560 analysis. This work was supported by NASA Astrobiology Institute Exobiology grant
561 #80NSSC19K0480; and by Caltech's Center for Environmental Microbial Interactions and
562 Division of Geological and Planetary Sciences. Fieldwork in South Africa by UFL was supported
563 by Woodward Fischer (Caltech) under grants from the NSF (IOS-1833247) and the Packard
564 Foundation.

565

566 **References**

- 567 1. Daims H. 2014. The Family *Nitrospiraceae*, p. 733–749. In Rosenberg, E, DeLong, EF,
568 Lory, S, Stackebrandt, E, Thompson, F (eds.), *The Prokaryotes: Other Major Lineages of*
569 *Bacteria and The Archaea*. Springer, Berlin, Heidelberg.
- 570 2. Garrity GM, Holt JG, Spieck E, Bock E, Johnson DB, Spring S, Schleifer K-H, Maki JS.
571 2001. Phylum BVIII. *Nitrospirae* phy. nov., p. 451–464. In Boone, DR, Castenholz, RW,
572 Garrity, GM (eds.), *Bergey's Manual of Systematic Bacteriology: Volume One : The*
573 *Archaea and the Deeply Branching and Phototrophic Bacteria*. Springer, New York.
- 574 3. Ehrlich S, Behrens D, Lebedeva E, Ludwig W, Bock E. 1995. A new obligately
575 chemolithoautotrophic, nitrite-oxidizing bacterium, *Nitrospira moscoviensis* sp. nov. and its
576 phylogenetic relationship. *Arch Microbiol* 164:16–23.
- 577 4. Watson SW, Bock E, Valois FW, Waterbury JB, Schlosser U. 1986. *Nitrospira marina* gen.
578 nov. sp. nov.: a chemolithotrophic nitrite-oxidizing bacterium. *Arch Microbiol* 144:1–7.
- 579 5. Daims H, Lebedeva EV, Pjevac P, Han P, Herbold C, Albertsen M, Jehmlich N, Palatinszky
580 M, Vierheilig J, Bulaev A, Kirkegaard RH, von Bergen M, Rattei T, Bendinger B, Nielsen
581 PH, Wagner M. 2015. Complete nitrification by *Nitrospira* bacteria. *Nature* 528:504–509.
- 582 6. van Kessel MAHJ, Speth DR, Albertsen M, Nielsen PH, Op den Camp HJM, Kartal B,
583 Jetten MSM, Lückner S. 2015. Complete nitrification by a single microorganism. *Nature*
584 <https://doi.org/10.1038/nature16459>.
- 585 7. Hippe H. 2000. *Leptospirillum* gen. nov. (ex Markosyan 1972), nom. rev., including
586 *Leptospirillum ferrooxidans* sp. nov. (ex Markosyan 1972), nom. rev. and *Leptospirillum*
587 *thermoferrooxidans* sp. nov. (Golovacheva et al. 1992). *Int J Syst* 50:501–503.
- 588 8. Henry EA, Devereux R, Maki JS, Gilmour CC, Woese CR, Mandelco L, Schauder R,
589 Remsen CC, MITCHELL R. 1994. Characterization of a new thermophilic sulfate-reducing
590 bacterium *Thermodesulfobacterium yellowstonii*, gen. nov. and sp. nov.: its phylogenetic
591 relationship to *Thermodesulfobacterium commune* and their origins deep within the
592 bacterial domain. *Arch Microbiol* 161:62–69.

- 593 9. Umezawa K, Kojima H, Kato Y, Fukui M. 2020. Disproportionation of inorganic sulfur
594 compounds by a novel autotrophic bacterium belonging to *Nitrospirota*. *Syst Appl*
595 *Microbiol* 43:126110.
- 596 10. Spring SS, Amann RR, Ludwig WW, Schleifer KHK, van Gemerden HH, Petersen NN.
597 1993. Dominating role of an unusual magnetotactic bacterium in the microaerobic zone of a
598 freshwater sediment. *Appl Environ Microbiol* 59:2397–2403.
- 599 11. Yu H, Leadbetter JR. 2020. Bacterial chemolithoautotrophy via manganese oxidation. 7816.
600 *Nature* 583:453–458.
- 601 12. Lingappa UF, Monteverde DR, Magyar JS, Valentine JS, Fischer WW. 2019. How
602 manganese empowered life with dioxygen (and vice versa). *Free Radic Biol Med* 140:113–
603 125.
- 604 13. Tebo BM, Johnson HA, McCarthy JK, Templeton AS. 2005. Geomicrobiology of
605 manganese(II) oxidation. *Trends Microbiol* 13:421–428.
- 606 14. Hansel C, Learman DR. 2015. Geomicrobiology of manganese, p. 401–452. *In* Ehrlich, HL,
607 Newman, DK, Kappler, A (eds.), *Ehrlich’s Geomicrobiology*, 6th ed. CRC Press.
- 608 15. Myers CR, Nealson KH. 1988. Bacterial manganese reduction and growth with manganese
609 oxide as the sole electron acceptor. *Science* 240:1319–1321.
- 610 16. Lovley DR, Phillips EJ. 1988. Novel mode of microbial energy metabolism: organic carbon
611 oxidation coupled to dissimilatory reduction of iron or manganese. *Appl Environ Microbiol*
612 54:1472–1480.
- 613 17. Leu AO, Cai C, McIlroy SJ, Southam G, Orphan VJ, Yuan Z, Hu S, Tyson GW. 2020.
614 Anaerobic methane oxidation coupled to manganese reduction by members of the
615 *Methanoperedenaceae*. 4. *ISME J* 14:1030–1041.
- 616 18. Beal EJ, House CH, Orphan VJ. 2009. Manganese- and iron-dependent marine methane
617 oxidation. *Science* 325:184–187.
- 618 19. Beijerinck M. 1913. Oxydation des mangancarbonates durch Bakterien und Schimmelpilze.
619 *Folia Microbiol (Delft)* 2:123–134.
- 620 20. Nealson KH, Tebo BM, Rosson RA. 1988. Occurrence and mechanisms of microbial
621 oxidation of manganese. *Adv Appl Microbiol* 33:279–318.
- 622 21. Thauer RK, Jungermann K, Decker K. 1977. Energy conservation in chemotrophic
623 anaerobic bacteria. *Bacteriol Rev* 41:100–180.
- 624 22. Bird LJ, Bonnefoy V, Newman DK. 2011. Bioenergetic challenges of microbial iron
625 metabolisms. *Trends Microbiol* 19:330–340.

- 626 23. Bowers RM, Kyrpides NC, Stepanauskas R, Harmon-Smith M, Doud D, Reddy TBK,
627 Schulz F, Jarett J, Rivers AR, Eloë-Fadrosch EA, Tringe SG, Ivanova NN, Copeland A,
628 Clum A, Becraft ED, Malmstrom RR, Birren B, Podar M, Bork P, Weinstock GM, Garrity
629 GM, Dodsworth JA, Yooseph S, Sutton G, Glöckner FO, Gilbert JA, Nelson WC, Hallam
630 SJ, Jungbluth SP, Etema TJG, Tighe S, Konstantinidis KT, Liu W-T, Baker BJ, Rattei T,
631 Eisen JA, Hedlund B, McMahon KD, Fierer N, Knight R, Finn R, Cochrane G, Karsch-
632 Mizrahi I, Tyson GW, Rinke C, Lapidus A, Meyer F, Yilmaz P, Parks DH, Murat Eren A,
633 Schriml L, Banfield JF, Hugenholtz P, Woyke T. 2017. Minimum information about a
634 single amplified genome (MISAG) and a metagenome-assembled genome (MIMAG) of
635 bacteria and archaea. *Nat Biotechnol* 35:725–731.
- 636 24. Jain C, Rodriguez-R LM, Phillippy AM, Konstantinidis KT, Aluru S. 2018. High
637 throughput ANI analysis of 90K prokaryotic genomes reveals clear species boundaries. *Nat*
638 *Commun* 9:5114.
- 639 25. Murray CS, Gao Y, Wu M. 2021. Re-evaluating the evidence for a universal genetic
640 boundary among microbial species. *Nat Commun* 12:4059.
- 641 26. Rodriguez-R LM, Konstantinidis KT. 2016. The enveomics collection: a toolbox for
642 specialized analyses of microbial genomes and metagenomes. *PeerJ Preprints* 4:e1900v1.
- 643 27. Parks DH, Chuvochina M, Waite DW, Rinke C, Skarshewski A, Chaumeil P-A,
644 Hugenholtz P. 2018. A standardized bacterial taxonomy based on genome phylogeny
645 substantially revises the tree of life. *Nat Biotechnol* 36:996–1004.
- 646 28. Parks DH, Chuvochina M, Rinke C, Mussig AJ, Chaumeil P-A, Hugenholtz P. 2021.
647 GTDB: an ongoing census of bacterial and archaeal diversity through a phylogenetically
648 consistent, rank normalized and complete genome-based taxonomy. *Nucleic Acids Res*
649 <https://doi.org/10.1093/nar/gkab776>.
- 650 29. Keffer JL, McAllister SM, Garber A, Hallahan BJ, Sutherland MC, Rozovsky S, Chan CS.
651 2021. Iron oxidation by a fused cytochrome-porin common to diverse iron-oxidizing
652 bacteria. *bioRxiv* 228056.
- 653 30. Jeans C, Singer SW, Chan CS, VerBerkmoes NC, Shah M, Hettich RL, Banfield JF, Thelen
654 MP. 2008. Cytochrome 572 is a conspicuous membrane protein with iron oxidation activity
655 purified directly from a natural acidophilic microbial community. *ISME J* 2:542–550.
- 656 31. Goltsman DSA, Denev VJ, Lefsrud M, Sun CL, Baker BJ, Land M, Shah MB, Hettich RL.
657 2009. Community genomic and proteomic analyses of chemoautotrophic iron-oxidizing
658 “*Leptospirillum rubarum*” (Group II) and “*Leptospirillum ferrodiazotrophum*” (Group III)
659 bacteria in acid mine drainage biofilms. *Appl Environ Microbiol* 75:4599–4615.
- 660 32. Lückner S, Wagner M, Maixner F, Pelletier E, Koch H, Vacherie B, Rattei T, Damsté JSS,
661 Spieck E, Le Paslier D, Daims H. 2010. A *Nitrospira* metagenome illuminates the
662 physiology and evolution of globally important nitrite-oxidizing bacteria. *Proc Natl Acad*
663 *Sci USA* 107:13479–13484.

- 664 33. Munding AB, Lawson CE, Jetten MSM, Koch H, Lückner S. 2019. Cultivation and
665 transcriptional analysis of a canonical *Nitrospira* under stable growth conditions. *Front*
666 *Microbiol* 10:1325.
- 667 34. Berg IA. 2011. Ecological aspects of the distribution of different autotrophic CO₂ fixation
668 pathways. *Appl Environ Microbiol* 77:1925–1936.
- 669 35. Chadwick GL, Hemp J, Fischer WW, Orphan VJ. 2018. Convergent evolution of unusual
670 complex I homologs with increased proton pumping capacity: energetic and ecological
671 implications. *ISME J* 12:2668–2680.
- 672 36. Brandt U. 2006. Energy converting NADH:quinone oxidoreductase (complex I). *Annu Rev*
673 *Biochem* 75:69–92.
- 674 37. Degli Esposti M, Martinez Romero E. 2016. A survey of the energy metabolism of
675 nodulating symbionts reveals a new form of respiratory complex I. *FEMS Microbiol Ecol*
676 92:fiw084.
- 677 38. Lewis WH, Tahon G, Geesink P, Sousa DZ, Ettema TJG. 2020. Innovations to culturing the
678 uncultured microbial majority. *Nat Rev Microbiol* 1–16.
- 679 39. Thrash JC. 2021. Towards culturing the microbe of your choice. *Environ Microbiol Rep*
680 13:36–41.
- 681 40. Uramoto G-I, Morono Y, Tomioka N, Wakaki S, Nakada R, Wagai R, Uesugi K, Takeuchi
682 A, Hoshino M, Suzuki Y, Shiraishi F, Mitsunobu S, Suga H, Takeichi Y, Takahashi Y,
683 Inagaki F. 2019. Significant contribution of subseafloor microparticles to the global
684 manganese budget. *Nat Commun* 10:1–10.
- 685 41. Richardson DJ, Butt JN, Fredrickson JK, Zachara JM, Shi L, Edwards MJ, White G, Baiden
686 N, Gates AJ, Marritt SJ, Clarke TA. 2012. The ‘porin–cytochrome’ model for microbe-to-
687 mineral electron transfer. *Mol Microbiol* 85:201–212.
- 688 42. Shi L, Dong H, Reguera G, Beyenal H, Lu A, Liu J, Yu H-Q, Fredrickson JK. 2016.
689 Extracellular electron transfer mechanisms between microorganisms and minerals. *Nat Rev*
690 *Microbiol* 14:651–662.
- 691 43. He S, Barco RA, Emerson D, Roden EE. 2017. Comparative genomic analysis of
692 neutrophilic iron(II) oxidizer genomes for candidate genes in extracellular electron transfer.
693 *Front Microbiol* 8:1584.
- 694 44. Luther III GW. 2005. Manganese(II) oxidation and Mn(IV) reduction in the environment—
695 two one-electron transfer steps versus a single two-electron step. *Geomicrobiol J* 22:195–
696 203.
- 697 45. Medina M, Rizo A, Dinh D, Chau B, Omidvar M, Juarez A, Ngo J, Johnson HA. 2018.
698 MopA, the Mn oxidizing protein from *Erythrobacter* sp. SD-21, requires heme and NAD⁺
699 for Mn(II) oxidation. *Front Microbiol* 9:2671.

- 700 46. Tebo BM, Geszvain K, Lee S-W. 2010. The molecular geomicrobiology of bacterial
701 manganese (II) oxidation, p. 285–308. *In* Geomicrobiology: Molecular and Environmental
702 Perspective. Springer.
- 703 47. Tebo BM, Bargar JR, Clement BG, Dick GJ, Murray KJ, Parker D, Verity R, Webb SM.
704 2004. Biogenic manganese oxides: properties and mechanisms of formation. *Annu Rev*
705 *Earth Planet Sci* 32:287–328.
- 706 48. Brouwers GJ, Vijgenboom E, Corstjens PLAM, De Vrind JPM, De Vrind-De Jong EW.
707 2000. Bacterial Mn²⁺ oxidizing systems and multicopper oxidases: an
708 overview of mechanisms and functions. *Geomicrobiol J* 17:1–24.
- 709 49. Emerson D, Fleming EJ, McBeth JM. 2010. Iron-oxidizing bacteria: an environmental and
710 genomic perspective. *Annu Rev Microbiol* 64:561–583.
- 711 50. Kappler A, Emerson D, Gralnick JA, Roden EE, Muehe EM. 2015. Geomicrobiology of
712 iron, p. 343–400. *In* Ehrlich's Geomicrobiology, 6th ed. CRC Press.
- 713 51. Bolyen E, Rideout JR, Dillon MR, Bokulich NA, Abnet CC, Al-Ghalith GA, Alexander H,
714 Alm EJ, Arumugam M, Asnicar F, Bai Y, Bisanz JE, Bittinger K, Brejnrod A, Brislawn CJ,
715 Brown CT, Callahan BJ, Caraballo-Rodríguez AM, Chase J, Cope EK, Da Silva R, Diener
716 C, Dorrestein PC, Douglas GM, Durall DM, Duvallet C, Edwardson CF, Ernst M, Estaki
717 M, Fouquier J, Gauglitz JM, Gibbons SM, Gibson DL, Gonzalez A, Gorlick K, Guo J,
718 Hillmann B, Holmes S, Holste H, Huttenhower C, Huttley GA, Janssen S, Jarmusch AK,
719 Jiang L, Kaehler BD, Kang KB, Keefe CR, Keim P, Kelley ST, Knights D, Koester I,
720 Kosciulek T, Kreps J, Langille MGI, Lee J, Ley R, Liu Y-X, Loftfield E, Lozupone C,
721 Maher M, Marotz C, Martin BD, McDonald D, McIver LJ, Melnik AV, Metcalf JL,
722 Morgan SC, Morton JT, Naimey AT, Navas-Molina JA, Nothias LF, Orchanian SB,
723 Pearson T, Peoples SL, Petras D, Preuss ML, Pruesse E, Rasmussen LB, Rivers A, Robeson
724 MS, Rosenthal P, Segata N, Shaffer M, Shiffer A, Sinha R, Song SJ, Spear JR, Swafford
725 AD, Thompson LR, Torres PJ, Trinh P, Tripathi A, Turnbaugh PJ, Ul-Hasan S, van der
726 Hooft JJJ, Vargas F, Vázquez-Baeza Y, Vogtmann E, von Hippel M, Walters W, Wan Y,
727 Wang M, Warren J, Weber KC, Williamson CHD, Willis AD, Xu ZZ, Zaneveld JR, Zhang
728 Y, Zhu Q, Knight R, Caporaso JG. 2019. Reproducible, interactive, scalable and extensible
729 microbiome data science using QIIME 2. *Nat Biotechnol* 37:852–857.
- 730 52. Callahan BJ, McMurdie PJ, Rosen MJ, Han AW, Johnson AJA, Holmes SP. 2016.
731 DADA2: High-resolution sample inference from Illumina amplicon data. *Nat Methods*
732 13:581–583.
- 733 53. Quast C, Pruesse E, Yilmaz P, Gerken J, Schweer T, Yarza P, Peplies J, Glöckner FO.
734 2013. The SILVA ribosomal RNA gene database project: improved data processing and
735 web-based tools. *Nucleic Acids Res* 41:D590-6.
- 736 54. Sadaiappan B, PrasannaKumar C, Nambiar VU, Subramanian M, Gauns MU. 2021. Meta-
737 analysis cum machine learning approaches address the structure and biogeochemical
738 potential of marine copepod associated bacteriobiomes. *Sci Rep* 11:3312.

- 739 55. Arkin AP, Cottingham RW, Henry CS, Harris NL, Stevens RL, Maslov S, Dehal P, Ware
740 D, Perez F, Canon S, Sneddon MW, Henderson ML, Riehl WJ, Murphy-Olson D, Chan SY,
741 Kamimura RT, Kumari S, Drake MM, Brettin TS, Glass EM, Chivian D, Gunter D, Weston
742 DJ, Allen BH, Baumohl J, Best AA, Bowen B, Brenner SE, Bun CC, Chandonia J-M, Chia
743 J-M, Colasanti R, Conrad N, Davis JJ, Davison BH, DeJongh M, Devoid S, Dietrich E,
744 Dubchak I, Edirisinghe JN, Fang G, Faria JP, Frybarger PM, Gerlach W, Gerstein M,
745 Greiner A, Gurtowski J, Haun HL, He F, Jain R, Joachimiak MP, Keegan KP, Kondo S,
746 Kumar V, Land ML, Meyer F, Mills M, Novichkov PS, Oh T, Olsen GJ, Olson R, Parrello
747 B, Pasternak S, Pearson E, Poon SS, Price GA, Ramakrishnan S, Ranjan P, Ronald PC,
748 Schatz MC, Seaver SMD, Shukla M, Sutormin RA, Syed MH, Thomason J, Tintle NL,
749 Wang D, Xia F, Yoo H, Yoo S, Yu D. 2018. KBase: The United States Department of
750 Energy systems biology knowledgebase. *Nat Biotechnol* 36:566–569.
- 751 56. Bolger AM, Lohse M, Usadel B. 2014. Trimmomatic: a flexible trimmer for Illumina
752 sequence data. *Bioinformatics* 30:2114–2120.
- 753 57. Bankevich A, Nurk S, Antipov D, Gurevich AA, Dvorkin M, Kulikov AS, Lesin VM,
754 Nikolenko SI, Pham S, Prjibelski AD, Pyshkin AV, Sirotkin AV, Vyahhi N, Tesler G,
755 Alekseyev MA, Pevzner PA. 2012. SPAdes: a new genome assembly algorithm and its
756 applications to single-cell sequencing. *J Comput Biol* 19:455–477.
- 757 58. Aziz RK, Bartels D, Best AA, DeJongh M, Disz T, Edwards RA, Formsma K, Gerdes S,
758 Glass EM, Kubal M, Meyer F, Olsen GJ, Olson R, Osterman AL, Overbeek RA, McNeil
759 LK, Paarmann D, Paczian T, Parrello B, Pusch GD, Reich C, Stevens R, Vassieva O,
760 Vonstein V, Wilke A, Zagnitko O. 2008. The RAST Server: rapid annotations using
761 subsystems technology. *BMC Genom* 9:75.
- 762 59. Overbeek R, Olson R, Pusch GD, Olsen GJ, Davis JJ, Disz T, Edwards RA, Gerdes S,
763 Parrello B, Shukla M, Vonstein V, Wattam AR, Xia F, Stevens R. 2014. The SEED and the
764 Rapid Annotation of microbial genomes using Subsystems Technology (RAST). *Nucleic
765 Acids Res* 42:D206-214.
- 766 60. Brettin T, Davis JJ, Disz T, Edwards RA, Gerdes S, Olsen GJ, Olson R, Overbeek R,
767 Parrello B, Pusch GD, Shukla M, Thomason JA, Stevens R, Vonstein V, Wattam AR, Xia
768 F. 2015. RASTtk: a modular and extensible implementation of the RAST algorithm for
769 building custom annotation pipelines and annotating batches of genomes. *Sci Rep* 5:8365.
- 770 61. Agarwala R, Barrett T, Beck J, Benson DA, Bollin C, Bolton E, Bourexis D, Brister JR,
771 Bryant SH, Canese K, Cavanaugh M, Charowhas C, Clark K, Dondoshansky I, Feolo M,
772 Fitzpatrick L, Funk K, Geer LY, Gorelenkov V, Graeff A, Hlavina W, Holmes B, Johnson
773 M, Kattman B, Khotomlianski V, Kimchi A, Kimelman M, Kimura M, Kitts P, Klimke W,
774 Kotliarov A, Krasnov S, Kuznetsov A, Landrum MJ, Landsman D, Lathrop S, Lee JM,
775 Leubsdorf C, Lu Z, Madden TL, Marchler-Bauer A, Malheiro A, Meric P, Karsch-Mizrachi
776 I, Mnev A, Murphy T, Orris R, Ostell J, O’Sullivan C, Palanigobu V, Panchenko AR, Phan
777 L, Pierov B, Pruitt KD, Rodarmer K, Sayers EW, Schneider V, Schoch CL, Schuler GD,
778 Sherry ST, Siyan K, Soboleva A, Sousoff V, Starchenko G, Tatusova TA, Thibaud-Nissen
779 F, Todorov K, Trawick BW, Vakarov D, Ward M, Yaschenko E, Zasytkin A, Zbicz K.

- 780 2018. Database resources of the National Center for Biotechnology Information. *Nucleic*
781 *Acids Res* 46:D8–D13.
- 782 62. Eren AM, Esen ÖC, Quince C, Vineis JH, Morrison HG, Sogin ML, Delmont TO. 2015.
783 Anvi'o: an advanced analysis and visualization platform for 'omics data. *PeerJ* 3:e1319.
- 784 63. Camacho C, Coulouris G, Avagyan V, Ma N, Papadopoulos J, Bealer K, Madden TL. 2009.
785 BLAST+: architecture and applications. *BMC Bioinform* 10:421.
- 786 64. Pruitt KD, Tatusova T, Brown GR, Maglott DR. 2012. NCBI Reference Sequences
787 (RefSeq): current status, new features and genome annotation policy. *Nucleic Acids Res*
788 40:D130–D135.
- 789 65. Edgar RC. 2004. MUSCLE: multiple sequence alignment with high accuracy and high
790 throughput. *Nucleic Acids Res* 32:1792–1797.
- 791 66. Federhen S. 2012. The NCBI Taxonomy database. *Nucleic Acids Res* 40:D136–143.
- 792 67. Nayfach S, Roux S, Seshadri R, Udwy D, Varghese N, Schulz F, Wu D, Paez-Espino D,
793 Chen I-M, Huntemann M, Palaniappan K, Ladau J, Mukherjee S, Reddy TBK, Nielsen T,
794 Kirton E, Faria JP, Edirisinghe JN, Henry CS, Jungbluth SP, Chivian D, Dehal P, Wood-
795 Charlson EM, Arkin AP, Tringe SG, Visel A, Woyke T, Mouncey NJ, Ivanova NN,
796 Kyrpides NC, Eloe-Fadrosh EA. 2021. A genomic catalog of Earth's microbiomes. *Nat*
797 *Biotechnol* 39:499–509.
- 798 68. Parks DH, Imelfort M, Skennerton CT, Hugenholtz P, Tyson GW. 2015. CheckM:
799 assessing the quality of microbial genomes recovered from isolates, single cells, and
800 metagenomes. *Genome Res* 25:1043–1055.
- 801 69. Pruesse E, Peplies J, Glöckner FO. 2012. SINA: accurate high-throughput multiple
802 sequence alignment of ribosomal RNA genes. *Bioinformatics* 28:1823–1829.
- 803 70. Ludwig W, Strunk O, Westram R, Richter L, Meier H, Yadhukumar, Buchner A, Lai T,
804 Steppi S, Jobb G, Förster W, Brettske I, Gerber S, Ginhart AW, Gross O, Grumann S,
805 Hermann S, Jost R, König A, Liss T, Lüssmann R, May M, Nonhoff B, Reichel B, Strehlow
806 R, Stamatakis A, Stuckmann N, Vilbig A, Lenke M, Ludwig T, Bode A, Schleifer K-H.
807 2004. ARB: a software environment for sequence data. *Nucleic Acids Res* 32:1363–1371.
- 808 71. Ronquist F, Teslenko M, van der Mark P, Ayres DL, Darling A, Höhna S, Larget B, Liu L,
809 Suchard MA, Huelsenbeck JP. 2012. MrBayes 3.2: efficient Bayesian phylogenetic
810 inference and model choice across a large model space. *Syst Biol* 61:539–542.
- 811 72. Letunic I, Bork P. 2021. Interactive Tree Of Life (iTOL) v5: an online tool for phylogenetic
812 tree display and annotation. *Nucleic Acids Res* 49:W293–W296.

813
814

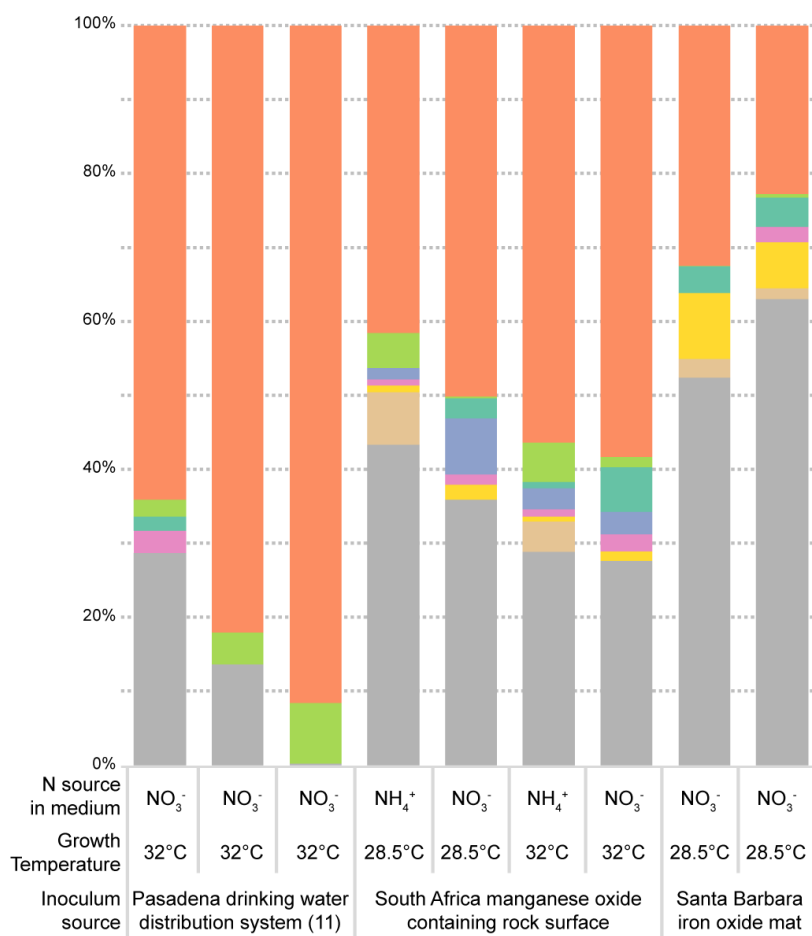
815 **Figures**

816

817 **Figure 1. Community analysis of manganese-oxidizing enrichment cultures using partial 16S**

818 **rRNA gene amplicon sequencing.** Taxonomic classification is based on the SILVA SSU rRNA

819 database v138. Detailed taxon relative abundances can be found in Supplementary Table 1.



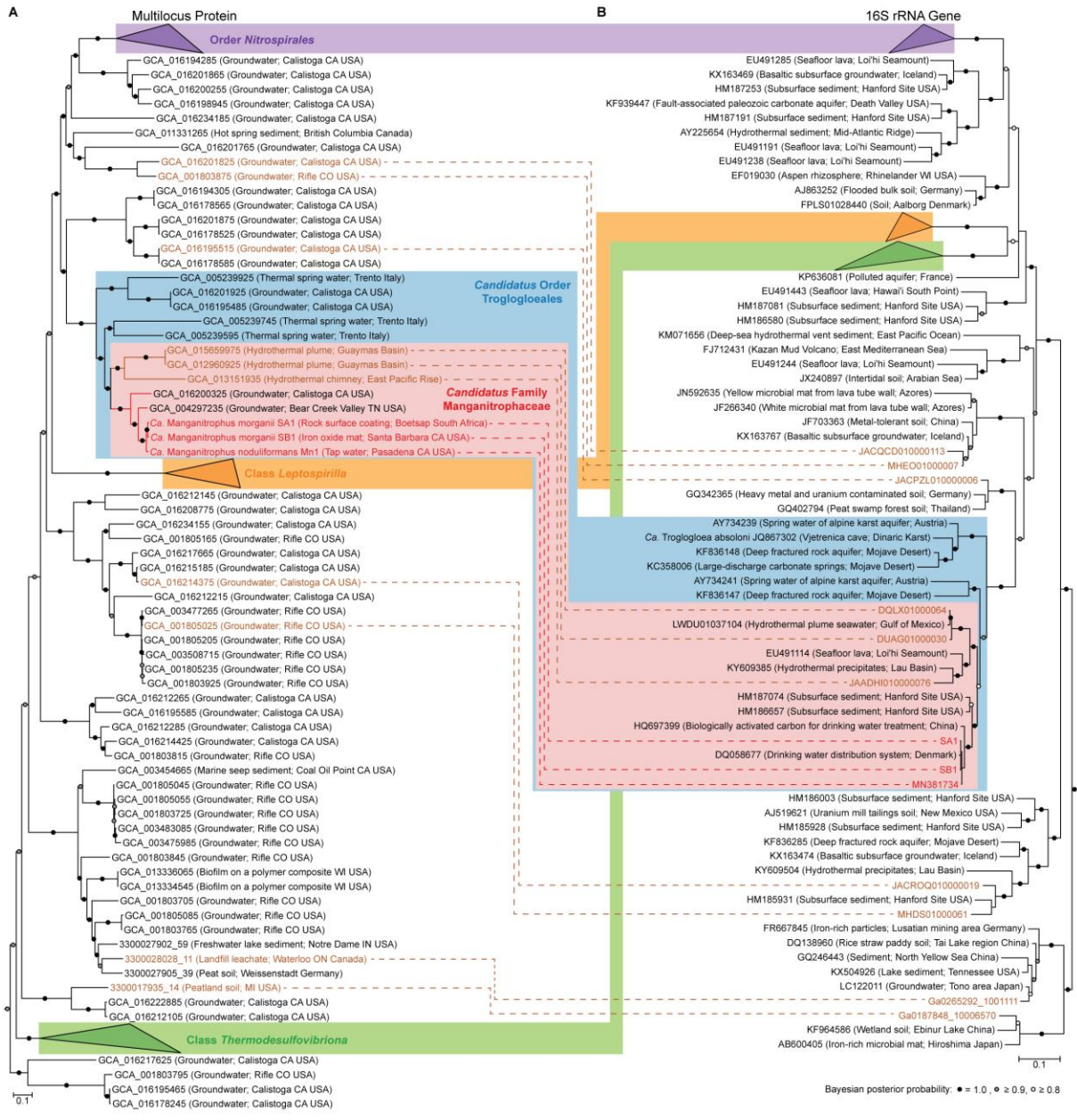
Taxa (SILVA taxonomy)

- *Candidatus* Manganitrophus noduliformans (p__Nitrospirota;c__Leptospirillia;o__Leptospirillales;f__Leptospirillaceae;g__Leptospirillum;s__uncultured_Nitrospirae)
- *Ramlibacter lithotrophicus* (p__Proteobacteria;c__Gammaproteobacteria;o__Burkholderiales;f__Comamonadaceae;g__Comamonadaceae;__)
- *Zavarziniales* (p__Proteobacteria;c__Alphaproteobacteria;o__Zavarziniales;f__uncultured;g__uncultured;s__uncultured_bacterium)
- *Hydrogenophaga* (p__Proteobacteria;c__Gammaproteobacteria;o__Burkholderiales;f__Comamonadaceae;g__Hydrogenophaga;__)
- *Burkholderiales* (p__Proteobacteria;c__Gammaproteobacteria;o__Burkholderiales;f__TRA3-20;g__TRA3-20;__)
- *Anaerolineaceae* (p__Chloroflexi;c__Anaerolineae;o__Anaerolineales;f__Anaerolineaceae;g__uncultured;__)
- *Pseudomonas* (p__Proteobacteria;c__Gammaproteobacteria;o__Pseudomonadales;f__Pseudomonadaceae;g__Pseudomonas;__)
- Others (<5% relative abundance in any enrichment culture)

820

821

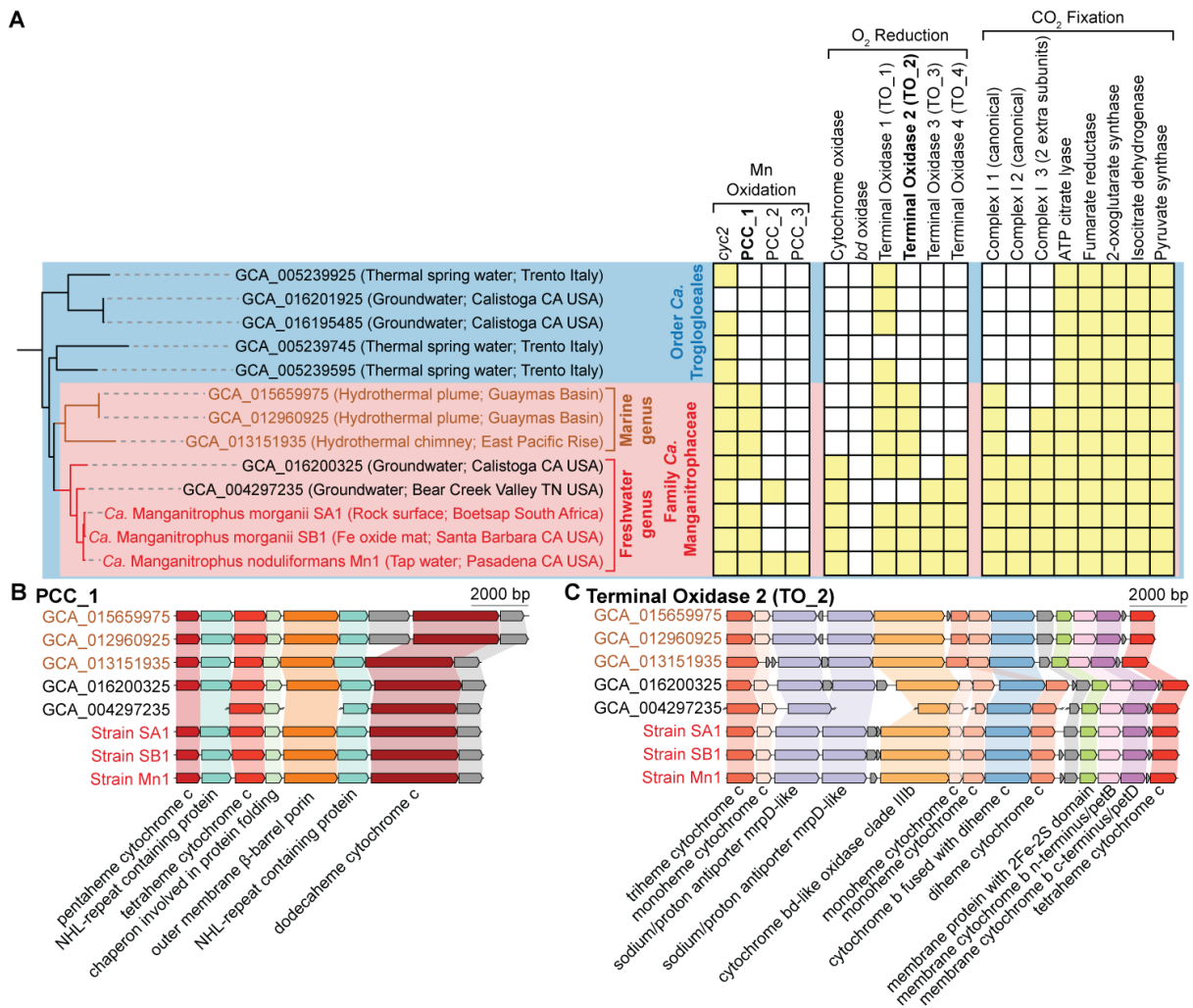
822 **Figure 2. Phylogenetic analysis of the bacterial phylum Nitrospirota.** **A**, Multilocus
 823 phylogram, based on a Bayesian analysis of 5040 aligned amino acid positions concatenated from
 824 120 bacterial protein markers. **B**, 16S rRNA gene phylogram, based on a Bayesian analysis of
 825 1508 aligned nucleotide positions. For both **A** and **B**, NCBI accession numbers or IMG contigs
 826 identifiers for the genome assemblies or 16S sequences are in the node names, with their source
 827 environments shown in brackets. Two phylograms can be linked by the genomes assemblies that
 828 contain 16S rRNA genes, with environmental metagenomes in brown and manganese-oxidizing
 829 enrichment cultures in red. Previously described taxonomic groups based on GTDB taxonomic
 830 classifications and the proposed taxonomic groups are color grouped.
 831



832

833

834 **Figure 3. Metabolic genes and gene clusters of interest in metagenome-assembled genomes**
 835 **representing the order *Candidatus Troglodloales*.** **A**, The multilocus protein phylogram and
 836 the presence (yellow filled square) or absence (empty square) of genes and gene clusters of interest
 837 in the corresponding genomes. Putative functional assignments are proposed above the gene and
 838 gene cluster names. The phylogram (left) is extracted from Figure 2. **B**, **C**, Comparison of gene
 839 clusters of porin cytochrome c 1 (PCC_1, **B**) and terminal oxidase 2 (TO_2, **C**), both restricted to
 840 the family *Candidatus Manganitrophaceae*. Members of the freshwater genus, *Candidatus*
 841 *Manganitrophus*, share similar gene arrangements which differ from those representing the
 842 candidatus marine genus (in brown).
 843

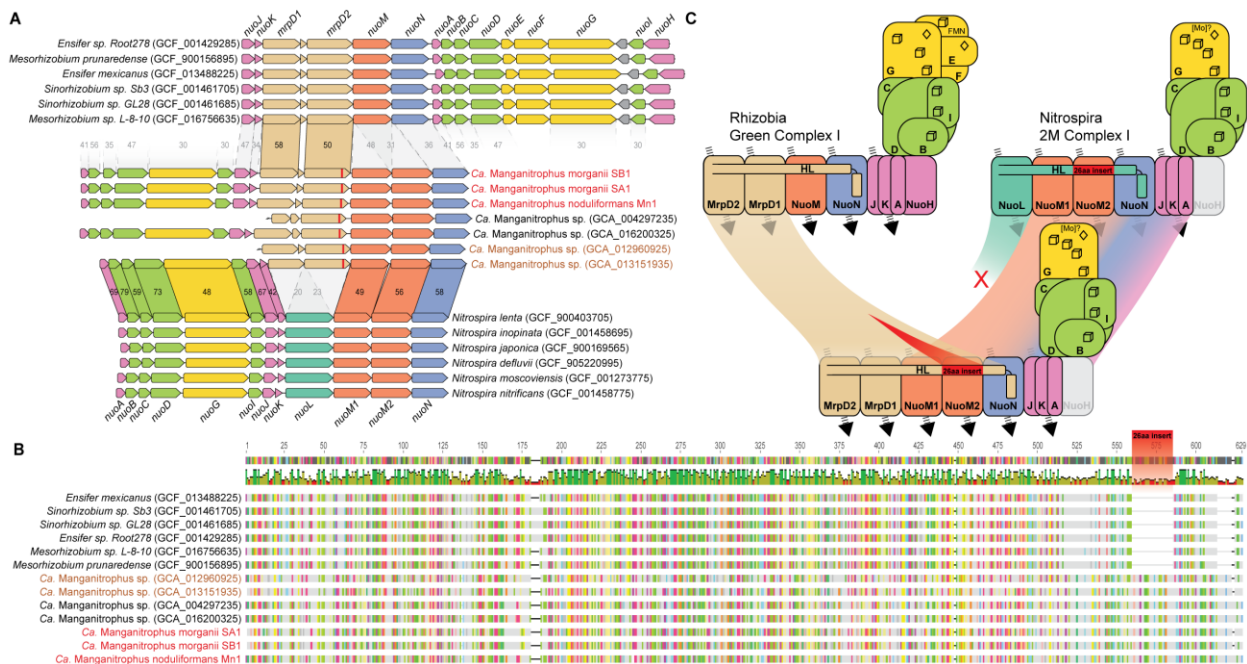


844

845

846 **Figure 4. Highly unusual Complex I (Complex_I_3) with two extra pumping subunits unique**
 847 **to *Candidatus* Manganitrophaceae.** **A**, Comparison of gene clusters of unusual Complex I with
 848 extra pumping subunits in *Ca. Manganitrophus* (middle) with their closest homologs in rhizobia
 849 (top) and *Nitrospira* (bottom). Homologs are connected between the 3 different organism clades,
 850 with values representing the average amino acid identities of proteins between the clades. NCBI
 851 accession numbers for the genome assemblies are included in brackets in the organism names. **B**,
 852 Sequence alignment of MrpD2 in Complex_I_3 in *Ca. Manganitrophaceae* reveals a 26 amino acid
 853 insert (red), compared to their closest homologs in rhizobia. **C**, Sequence comparisons reveal that
 854 Complex_I_3 in *Ca. Manganitrophaceae* is likely a hybrid between the Green Complex I in
 855 rhizobia and the 2M Complex I in *Nitrospira*. Given their sequence similarities, the two MrpD's
 856 in Complex_I_3 could be derived from rhizobia, whereas the other components in Complex_I_3
 857 could be derived from *Nitrospira*. The 1-2 extra pumping subunits in these unusual Complex I
 858 could enable translocation of a total of 5-6 protons or ions (as indicated by dashed arrows),
 859 compared to the 4 protons translocated by the canonical Complex I.

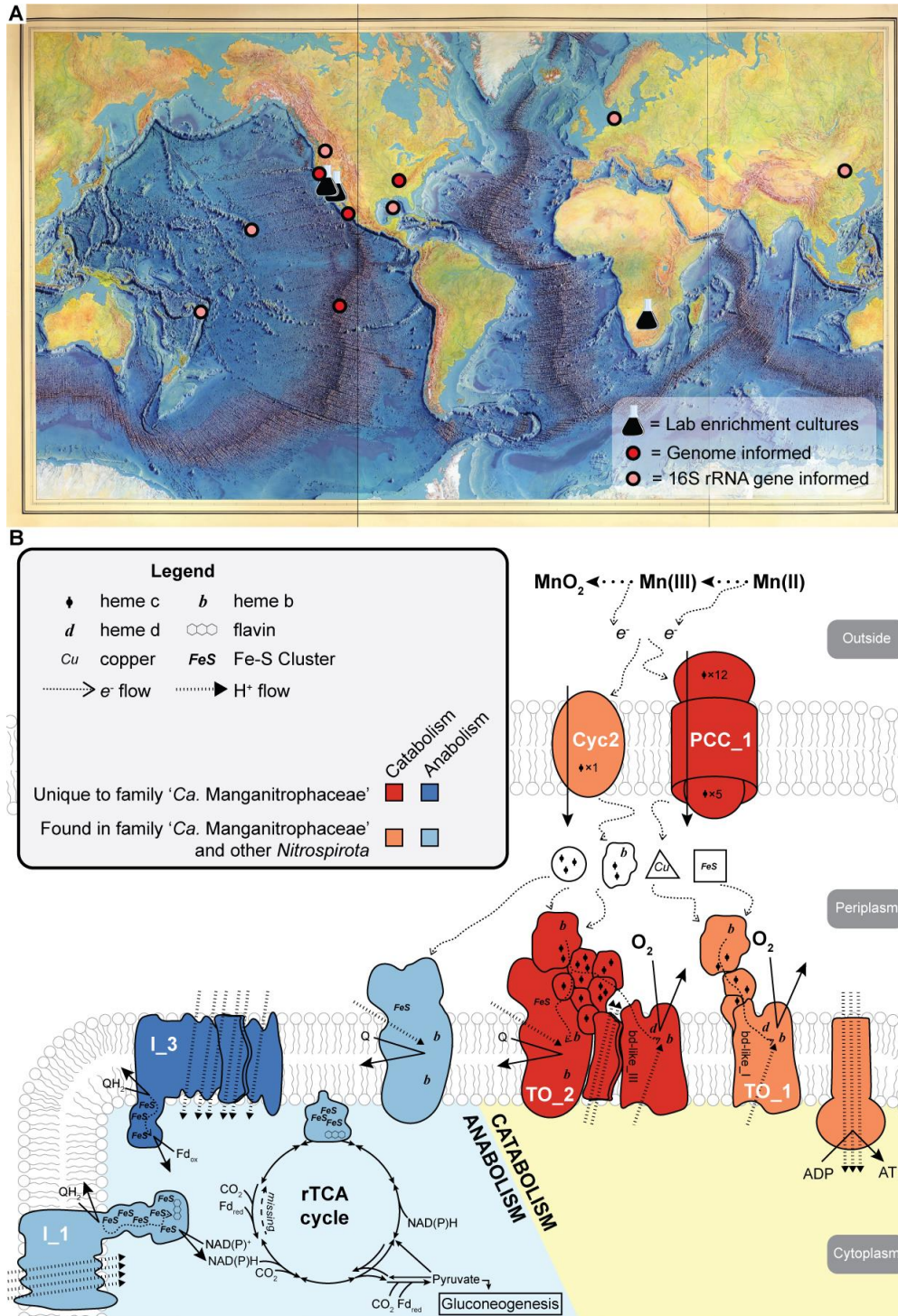
860



861

862

863 **Figure 5. Global distribution of *Candidatus* Manganitrophaceae and key proteins and**
 864 **complexes putatively facilitating manganese metabolism. A, Distribution of cultures,**
 865 **metagenome-assembled genomes, and phylotypes representing *Ca.* Manganitrophaceae implies**
 866 **their worldwide reach in freshwater and marine environments. B, Cell diagram shows proposed**
 867 **proteins and complexes of interest to manganese chemolithoautotrophy, as deduced from**
 868 **representative genomes.**
 869



870